

Comparison of matching layers for automotive radome design

F. Fitzek¹, R. H. Rasshofer¹, and E. M. Biebl²

¹BMW Group Research and Technology, Munich, Germany

²Technische Universität München – Fachgebiet Höchstfrequenztechnik, Munich, Germany

Abstract. Hidden integration of 79 GHz sensors behind plastic and painted fascia represents a challenging task since both electromagnetic and car body design constraints have to be met. This paper compares different possibilities for low-cost integration of radar sensors. Based on a model for stratified media, a study of the most important parameters such as bandwidth, angle and tolerances is shown. Our results suggest that for plastic fascia, the requirements of future radar sensors can be met with low-cost matching. Even with metallic paints, the requirements imposed by modern 79 GHz radar sensors can be met under certain conditions.

1 Introduction

Automotive radar systems, first introduced on the customer market in the late 1990s, show a steady trend from comfort (Advanced Driver Assistance, short ADAS) to safety oriented vehicle functions (Active Safety, short AS). Radar-based systems tend to address scenarios of growing complexity, targeting urban or city traffic rather than highway scenarios, which were the main application in recent years. Resolution in range, azimuth angle and target velocity is the key feature to deal with demanding scenarios of high complexity and high dynamics (Rasshofer, 2007). In the European Union, a new frequency band from 77 to 81 GHz – the 79 GHz band – has been allocated to enable future ADAS and AS systems replacing the previously used 24 GHz ultrawide band radar sensors. To start the development of 79 GHz band technology, the European funded project “Radar on Chip for Cars” (short RoCC) started in fall 2008 (RoCC, 2009).

Integration of 79 GHz sensors into modern cars represents a challenging task since electromagnetic and car body design constraints have to be met simultaneously. This problem is even more evident when more than one sensor has to be integrated, because hidden integration of the sensors behind a plastic bumper is often required. As is clear from

both theoretical investigations and from previous experience with 76 GHz radar systems, operation of these sensors behind painted, plastic fascia will lead to performance degradation if no optimization of the stratified radome structures is performed. In the millimetre wave regime, the electromagnetic field propagates quasi-optically, which results in high reflection and loss factors for obstacles or media in the line-of-sight. This is the case if the radar sensor is to be integrated in the bumper or behind other fascia of the car.

The performance degradation is due to the reflections between the bumper and the sensor. The bumper consists generally of a substrate and some layers of paint. This paper shows a detailed analysis of important electromagnetic radome properties like bandwidth, angle and tolerances for substrate only and painted substrates. Additionally, the cost of integration should be at a minimum, hence this paper considers low-cost matching possibilities for hidden integration of radar sensors.

2 Mathematical model

The electromagnetic theory of the fields in stratified media can be derived from the plane wave assumption and the boundary conditions of electromagnetic waves (time-harmonic convention $e^{j\omega t}$). In Kurt Altenburg (1953) this theory is derived. It can be found today in many books for optics, electromagnetics or microwave theory (Hecht, 2005). In the case of perpendicular incidence of a TE-wave (derivation for TM-waves accordingly) forward- and backward waves are defined, which summarize all waves in the same direction (important difference to other approaches). The complete derivation can be found in Hecht (2005) and a summary of it in Fitzek and Rasshofer (2009). For each layer i with the material parameters n_i as the index of refraction ($k_i = \omega/c_0 n_i$ respectively), d_i as the thickness, and Z_i as the wave impedance of the semi-infinite layer the following characteristic matrix can be derived.



Correspondence to: F. Fitzek
(frerk.fitzek@bmw.de)

$$[\mathbf{M}^i] = \begin{bmatrix} m_{11}^i & m_{12}^i \\ m_{21}^i & m_{22}^i \end{bmatrix} \quad (1)$$

$$= \begin{bmatrix} \cos(k_i d_i) & j Z_i \sin(k_i d_i) \\ j \frac{1}{Z_i} \sin(k_i d_i) & \cos(k_i d_i) \end{bmatrix} \quad (2)$$

The amplitude transmission- and reflection factors of the layer i embedded between semi-infinite layers $i-1$ and $i+1$ are defined as

$$r = \frac{Z_{i+1} m_{11}^i + m_{12}^i - Z_{i+1} Z_{i-1} m_{21}^i - Z_{i-1} m_{22}^i}{Z_{i+1} m_{11}^i + m_{12}^i + Z_{i+1} Z_{i-1} m_{21}^i + Z_{i-1} m_{22}^i} \quad (3)$$

$$t = \frac{2 Z_{i+1}}{Z_{i+1} m_{11}^i + m_{12}^i + Z_{i+1} Z_{i-1} m_{21}^i + Z_{i-1} m_{22}^i} \quad (4)$$

With these equations, the transmission and reflection factor can be derived using the loads and the characteristic matrix \mathbf{M}^i . For a multilayer media, the characteristic media matrices have to be multiplied in the right order.

3 Theory and practice of matching

The theory of matching is well known from transmission line theory. The aim is always to get a high transmission next to a low reflection (power matching). The losses in the material can't be compensated, which results in a decreased transmission. For semi-infinite layers, the methods shown here can be used as well. Nevertheless, for mm-wave applications the constraints of matching should be carefully considered (e.g. Fitzek and Raschofer, 2009).

For a bumper consistent of one layer of substrate and several layers of paint, there exists different options for matching. One is to optimize the thickness of the substrate. For a homogeneous material this results in a thickness of multiple of half-wavelengths. For stratified media, the solution can be found with minimization of the reflection coefficient through the mathematical model. This matching has only one degree of freedom – the decreased thickness of the substrate material. Another possibility is an additional matching layer which is placed directly onto the bumper. This material can have a desired thickness and relative permittivity, hence has two degrees of freedom. One could also consider artificial structures or even metamaterials as an additional matching layer, but as mentioned above, low-cost matching is the focus in this paper, hence these options are not considered.

The third matching option is a combination of these two matching methods. Therefore, a structure (e.g. rib profile) is assembled into the substrate material of the bumper. Because the overall thickness stays constant, this matching method has only two degrees of freedom (depth and relative permittivity of the integrated structure). Figure 1 depicts the different possibilities. For all matching methods the mathematical model can be used to calculate the optimal values for the desired matching. Therefore, an optimization algorithm based on a direct search method is used. Two different simulations

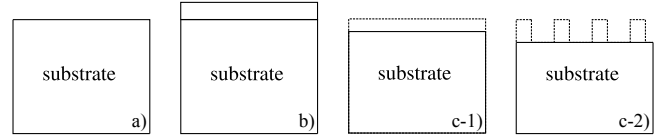


Fig. 1. (a) substrate material of bumper (no matching), (b) substrate with additional matching layer, (c-1) substrate with integrated matching layer (thickness optimization), (c-2) substrate with integrated matching layer (rib profile).

can be performed where the thickness and relative permittivity for the matching layer are optimized. This approach neglects the roughness of the material and assumes a non-magnetic, plane material.

For the additional matching layer, the bumper materials (substrate or paint) are *not* changed. On the other hand, for an integrated matching layer, the thickness of the substrate material is changed according to the thickness of this layer. This results in a decreased thickness for the substrate material of the bumper. With this integrated matching the integrated structure and the thickness optimization can be modeled. For the latter the relative permittivity is fixed to one, whereas it is a degree of freedom for the integrated structure.

3.1 Integrated matching structure

The integrated matching structure is a structured dielectric (e.g. rib profile) and can be any structure which fulfills the homogeneity limit of $p < \lambda/4$ with p as the cell size in the direction of propagation, in order to avoid parasitic scattering effects. For easy integration the rib profile is one possibility. There exists several methods to calculate the relative permittivity of such structures (Biber, 2003). Here a method based on transmission line models is used in which the resulting relative permittivity is described as the mean of the relative characteristic impedances ($Z' = \sqrt{\frac{\mu_r}{\epsilon_r}}$ with $\mu_r = 1$) of free space and the substrate depending on the ratio of ribs and bars. Hence, a relative permittivity between 1 and $\epsilon_{r,s}$ of the substrate can be reached.

$$\epsilon_r = \left(\frac{t_{\text{bar}} Z'_{\text{substrate}} + t_{\text{rib}} Z'_0}{t_{\text{bar}} + t_{\text{rib}}} \right)^{-2} \quad (5)$$

If the thickness of the ribs (t_{rib}) are predefined due to manufacturing constraints, one can easily calculate the thickness of the bars (t_{bar}) to reach the desired value for ϵ_r as calculated by the optimization algorithm.

Figure 2 shows the dependency of the relative permittivity versus the ratio of bars to ribs with constant rib thickness. It can be seen that the variation in relative permittivity for an increased bar thickness (resulting in higher ϵ_r values) is lower, than for smaller values of the bar thickness. This will be an important design possibility later on.

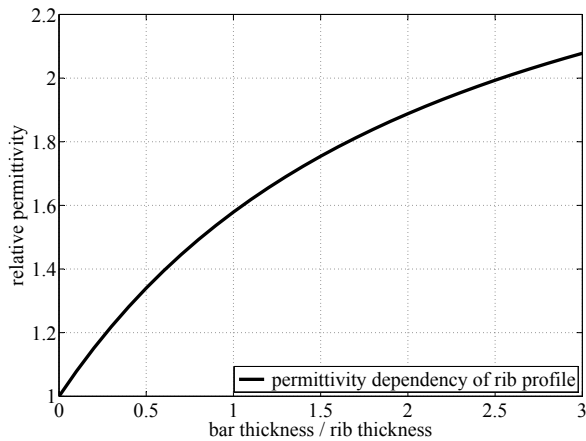


Fig. 2. Permittivity dependency of rib profile.

4 Comparison of matching layers

For the comparison of these different approaches the optimization algorithm is visualized by graphs with all possible degrees of freedom. This means that for all possible thickness of matching layer, all possible relative permittivities ϵ_r are shown. Obviously this can not be done for really all possibilities, so discrete values are chosen in steps of 0.1 for the relative permittivity.

This is done for one frequency $f = 78.5$ GHz and for the considered bandwidth $B = 76 - 81$ GHz. For the bandwidth the maximum reflection (meaning the worst case) within the band is considered for the evaluation. The best solution of the bandwidth analysis is taken for an angle variation in the range of ± 40 deg. With the more exact solution (ϵ_r stepsize 0.01) of the algorithm a tolerance analysis is shown with variations of $\sigma = \pm 0.1$ mm. For the additional matching layer the variation affects only the thickness of this layer. For the thickness optimization (integrated matching layer) the variation only affects the thickness of the substrate material of the bumper. The variation of the integrated structure (integrated matching layer) affects on the one hand the thickness of the substrate material and on the other hand ϵ_r in our case the thickness of the bars.

4.1 Additional matching layer for substrate

The results for an additional matching layer for the substrate material of the bumper (no paint considered yet) are depicted in Fig. 3a and b. In these figures the first (+), best (diamond) and last (x) graph are always highlighted to see the influence of increasing relative permittivity. The substrate material has a relative permittivity in the range of $\epsilon_{r,s} = 2.86 - 0.06i$ and a thickness of about $d_s = 3$ mm. Considering low-cost materials the relative permittivity for the matching layer is varied between $\epsilon_r = 1$ (initial condition) and $\epsilon_r = 3$. It can be seen that for a relative permittivity of $\epsilon_r = 2.6$ and a thickness of $d = 0.43$ mm the reflection can be decreased by about 45 dB

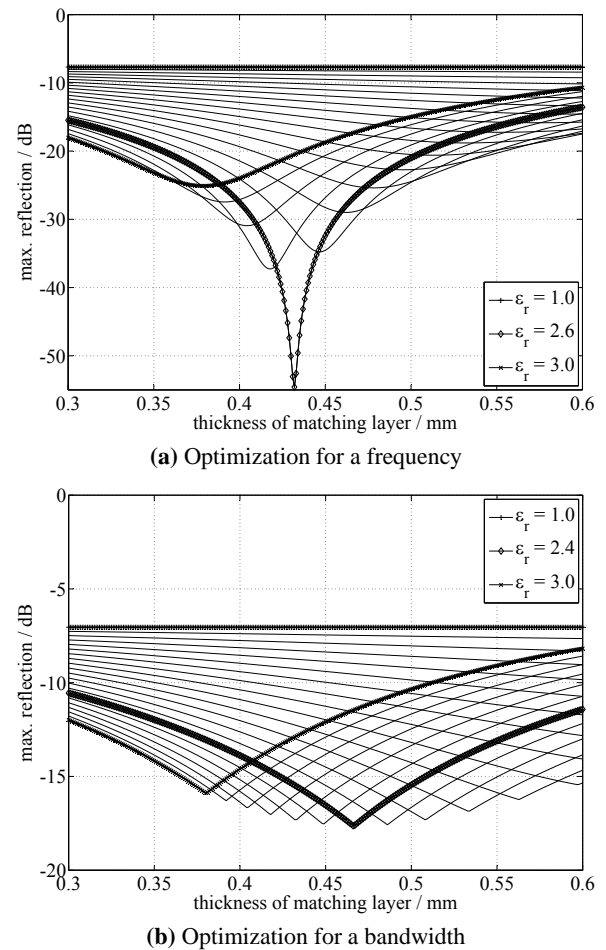


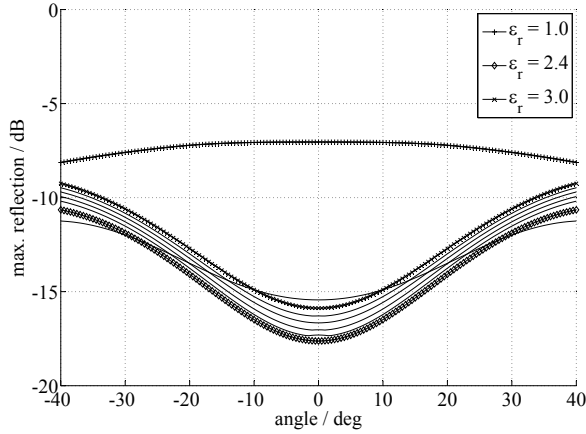
Fig. 3. Frequency and bandwidth analysis.

for one frequency ($f = 78.5$ GHz). Considering the maximum reflection within the band ($B = 76 - 81$ GHz) the improvement is about 10 dB, resulting in a maximum reflection of -17 dB. This is achieved for a relative permittivity of $\epsilon_r = 2.4$ and a thickness of $d = 0.47$ mm.

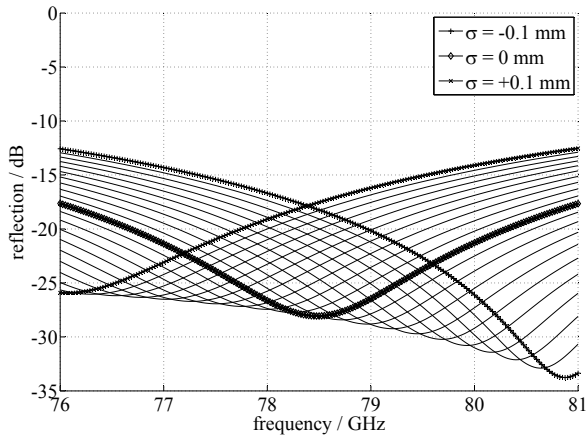
The angular dependency is depicted in Fig. 4a. Here the optimal values for the relative permittivity and thickness combination from the bandwidth analysis are used to show the behaviour. The combination mentioned before also gives the best result for the angular dependency. Hence, the maximum reflection coefficient within an angle of ± 40 deg is still below -10 dB. In Fig. 4b the reflection is shown over frequency. The maximum reflection coefficient of about -17 dB can be seen at the edges of the band (76/81 GHz) as calculated before. Next to that the tolerance analysis for a variation of $\sigma = \pm 0.1$ mm is shown. The maximum reflection is below -12 dB.

4.2 Integrated matching layer for substrate

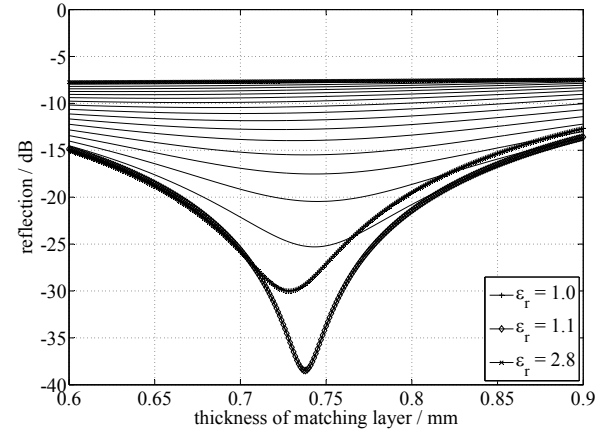
The results for an integrated matching layer for the substrate material of the bumper (again no paint considered) are



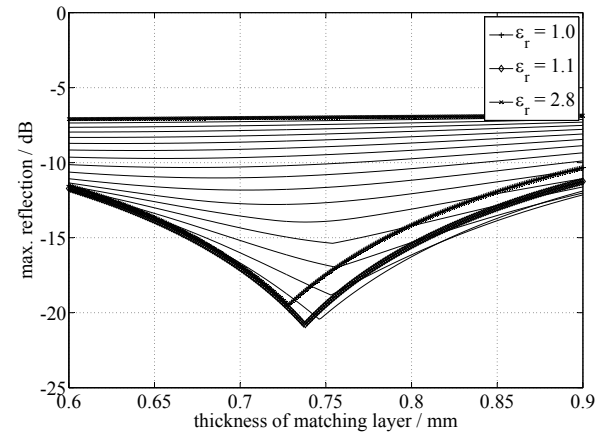
(a) Angular dependency analysis



(b) Tolerance analysis

Fig. 4. Angular and tolerance analysis.

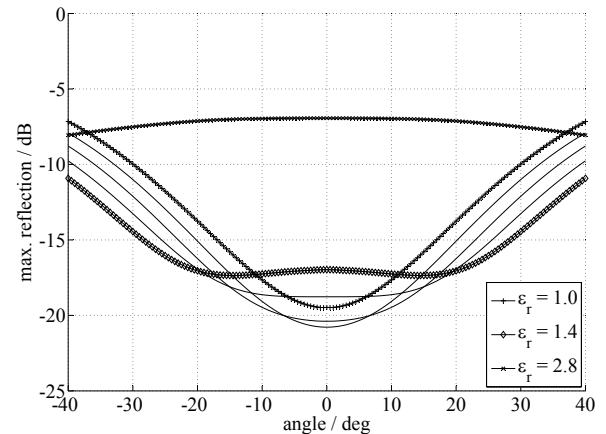
(a) Optimization for a frequency



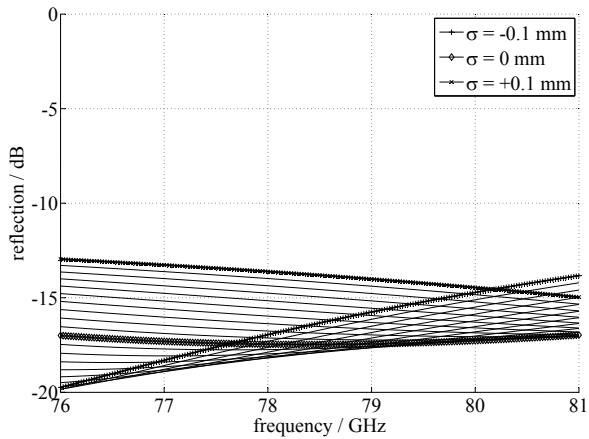
(b) Optimization for a bandwidth

Fig. 5. Frequency and bandwidth analysis.

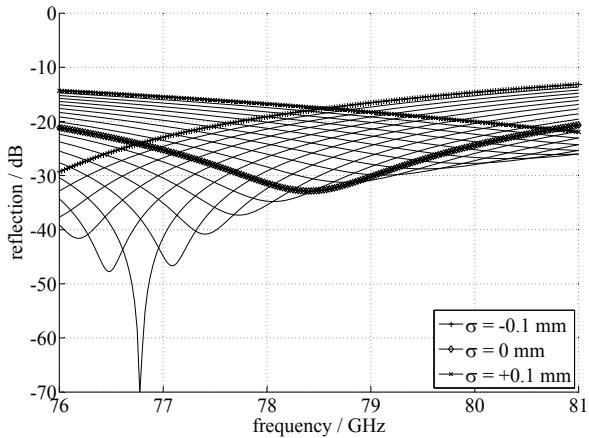
depicted in Fig. 5a and b. This is done for the same material like before. The only difference is the above mentioned reduction of the substrate material. In the figures $\epsilon_r = 1$ shows the results for a thickness optimization, because only the thickness of the matching layer is varied. This results in a decreased thickness of the substrate material of the bumper. The initial condition is represented by the relative permittivity of $\epsilon_r = 2.8$, which is nearly the same as the substrate material itself. The optimal solution for one frequency and for the bandwidth is $\epsilon_r = 1.1$ with a thickness of $d = 0.74$ mm. The maximum reflection within the band is about -21 dB, 4 dB lower than that of the additional matching layer. The angular dependency is depicted in Fig. 6. The solution of the bandwidth analysis shows no improvement concerning the maximum reflection within the angular range. Nevertheless for a smaller range (e.g. ± 30 deg) the maximum reflection would be below -10 dB. To cover the complete angular range one ends up with another solution, $\epsilon_r = 1.4$, which reduces the maximum reflection below -10 dB, but increases the reflection for 0 deg by about 2 dB. Concerning only the angular dependency this would be the optimal solution. This shows

**Fig. 6.** Angular analysis.

that already in this stage the meaning of “optimal” is not distinct. In the Sect. 4.3 this will be discussed. Nevertheless we have now two possible “optimal” solutions. The results of the tolerance analysis are shown in Fig. 7a for $\epsilon_r = 1.4$ and



(a) Tolerance analysis for a rel. permittivity of 1.4



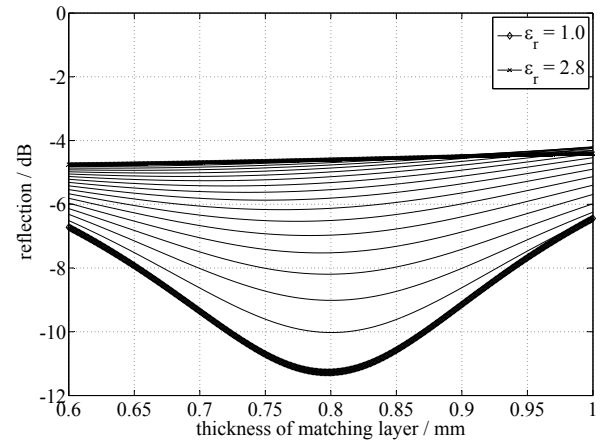
(b) Tolerance analysis for a rel. permittivity of 1.1

Fig. 7. Tolerance analysis.

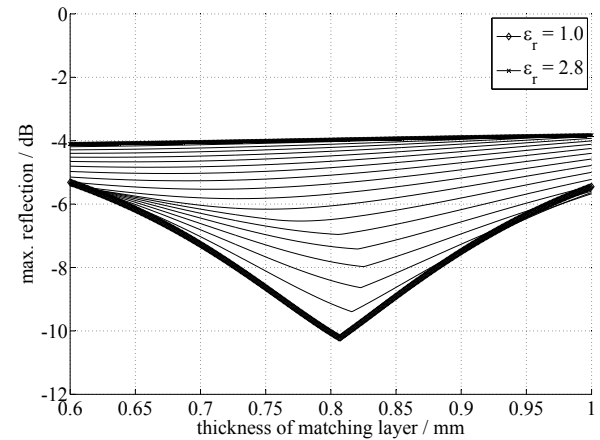
7b for $\epsilon_r = 1.1$. Here the before mentioned coherence between a higher permittivity and a smaller variation in relative permittivity can be seen.

4.3 Discussion of substrate materials

The analysis of the reflections coming from the bumper shows that one optimal solution can not be defined without knowing the sensor requirements. Nevertheless it is possible to define a cost function from sensor requirements which clearly defines the optimal solution. Together with the detailed analysis shown above the optimal parameters can hence be calculated. Additionally, the evaluation shows that the integrated matching layer is superior over the additional matching layer concerning maximum reflection within the bandwidth. Because this is a strong requirement for future radar sensors, the evaluation is focused on integrated matching layers in the following section.



(a) Optimization for a frequency



(b) Optimization for a bandwidth

Fig. 8. Frequency and bandwidth analysis.

4.4 Integrated matching layer for substrate and paint

The results for an integrated matching layer for the substrate material of the bumper with metallic paint (permittivity of metallic paint $\epsilon_r > 4$ – condition depends on the substrate's permittivity) are depicted in Fig. 9a and 9b. The substrate material is the same as before but with a slightly decreased thickness of $d_s = 2.7$ mm. Again, the integrated matching layer results in a reduction of the substrate material. In the figures $\epsilon_r = 1$ is coexistent for a thickness optimization and $\epsilon_r = 2.8$ represents the initial condition. The figures show that the reflections are increased for the substrate material with metallic paint. The optimal solution for one frequency and for the bandwidth is $\epsilon_r = 1$ with a thickness of $d = 0.81$ mm¹. The maximum reflection within the band is about -10 dB. The angular dependency is depicted in Fig. 9a for the best solutions of the bandwidth analysis. The maximum reflection within an angular range of ± 40 deg is about -4.5 dB. This can be optimized with a relative permittivity of $\epsilon_r = 1.6$ below -6 dB, but with higher reflections within the band.

¹For paints with $\epsilon_r < 4$ the optimal solution differs.

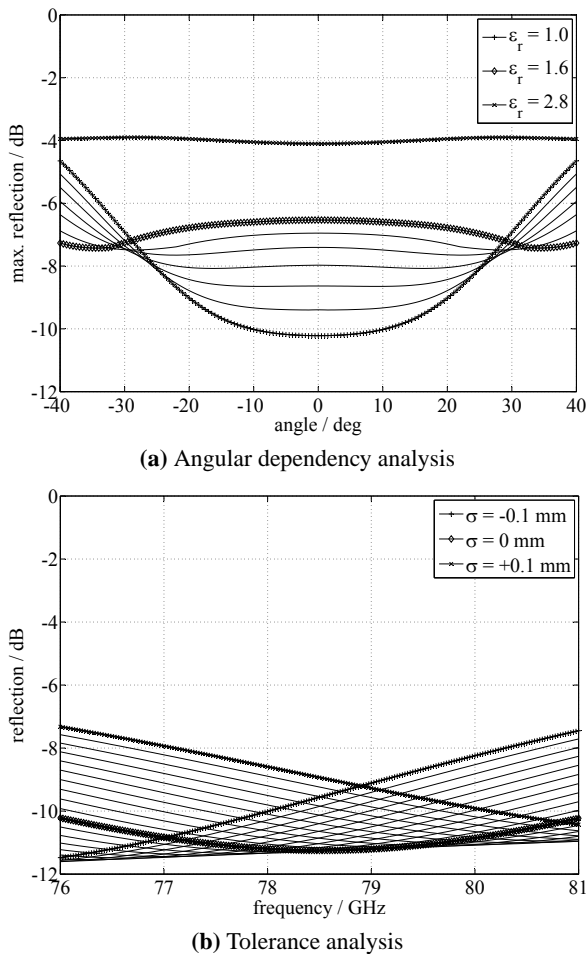


Fig. 9. Angular and tolerance analysis.

Nevertheless for a reduced angular range of $\pm 10^\circ$ the maximum reflection within the angular range and the bandwidth are below -10 dB. The tolerance analysis shows a maximum reflection below -7 dB. For $\sigma = 0$ mm the result of the bandwidth analysis can be checked with a maximum reflection within the band below -10 dB.

4.5 Discussion of painted materials

The evaluation of the different parameters show that it is possible to reduce the maximum reflection within the bandwidth below -10 dB even with metallic paints. Metallic paints have the highest permittivities of all paints, hence considering a worst case. It is clearly shown that the angular dependency and the tolerances play an important role for the design of an optimal matching layer. Again an "optimal" solution only exists for specific sensor requirements.

5 Conclusions

This paper compares different possibilities for low-cost integration of radar sensors for the 79 GHz band. The assumptions of the model described are a plane wave incident on a non-magnetic, plane material without roughness. It is shown for plastic fascia, that the bandwidth requirements $B = 76 - 81$ GHz, the angular requirements $\pm 40^\circ$ and tolerance influences $\sigma = \pm 0.1$ mm can be met coexistently with low-cost matching. This can be realized using a rib profile (integrated matching layer).

For painted fascia the bandwidth requirement can be met with a maximum reflection of below -10 dB. The thickness optimization (integrated matching layer) delivers the best solution considering the mentioned realization possibilities. Because the angular dependency and the tolerance analysis are based on this evaluation, they suffer from the requirement of 5 GHz bandwidth. Nevertheless the maximum reflection can be reduced below -10 dB under certain conditions. The optimisation of the angular dependency and the tolerance influence is considered for future work. An overall optimal solution can be found knowing the detailed requirements of future radar sensors.

Acknowledgements. The authors wish to thank the German Federal Ministry of Education and Research (BMBF) for the funding of the RoCC joint project.

References

- Alitalo, P., Luukkonen, O., Vehmas, J., and Tretyakov, S. A.: Impedance-Matched Microwave Lens, 7, 187–191, 2008.
- Biber, S., Richter, J., Martius, S., and Schmidt, L.-P.: Design of artificial dielectrics for anti-reflection-coatings, in: European Microwave Conference, 33rd, October 2003, pp. 1115–1118, 2003.
- Fitzek, F. and Raschofer, R. H.: Automotive Radome Design – Reflection Reduction in stratified media, *Antennas and Wireless Propagation Letters*, IEEE, 8, 2009.
- Hecht, E.: *Optik*, Oldenbourg Wissenschaftsverlag, 2005.
- Jones, E. and Cohn, S.: Surface matching of dielectric lenses, in: *Proc. IRE International Convention Record*, vol. 2, pp. 46–53, 1954.
- Kurt Altenburg, S. K.: Wellenausbreitung in geschichteten Medien bei senkrechtem Einfall [...], *Annalen der Physik*, 448, 1–43, 1953.
- Raschofer, R. H.: Functional Requirements of Future Automotive Radar Systems, in: *Proc. of the European Radar Conference*, Munich, Germany, 2007.
- RoCC press release, <http://www.eenova.de/news-presse/rocc/>, 2009.